JKAS
Journal of the Korean Astronomical Society
http://jkas.kas.org
eISSN: 2288-890X · pISSN: 1225-4614

JKAS (2023), **56**, 1, 91–96
doi: 10.5303/JKAS.2023.56.1.91

The First Multi-Frequency Synthesis Space-VLBI Observations of 0059+581 with Radioastron

Alexey Rudnitskiy[1,⋆], **Mikhail Shchurov**[1], **Taehyun Jung**[2], **and Marcello Giroletti**[3]

[1]Astro Space Center, Lebedev Physical Institute, Russian Academy of Sciences, Profsoyuznaya str. 84/32, Moscow, 117997, Russia
[2]Korea Astronomy and Space Science Institute, Yuseong-gu, Daejeon 34055, Republic of Korea
[3]INAF Istituto di Radioastronomia, via Gobetti 101, 40129 Bologna, Italy
⋆Corresponding Author: A. Rudnitskiy, arud@asc.rssi.ru

Received January 10, 2023; Accepted May 1, 2023; Published May 12, 2023

Abstract

In this paper, we describe the first multi-frequency synthesis observations of blazar 0059+581 made with the Radioastron space-ground interferometer in conjunction with the Korean VLBI Network (KVN), Medicina and Torun ground telescopes. We conducted these observations to assess the spaceground interferometer multi-frequency mode capability for the first time.

Keywords: techniques: interferometric — quasars: general — space vehicles: instruments

1. Introduction

Very long baseline radio interferometry (VLBI) with space radio telescope launches has demonstrated the aperture filling problem. In principle, this point is crucial for any VLBI observations related to detailed and high-quality imaging of cosmic sources. But it is more noticeable and critical for space-ground VLBI.

It is worthwhile to note that VLBI is moving rapidly towards the millimeter wavelength range as a consequence of modern astronomical problems and tasks. On Earth, long-term observations in the millimeter range are accompanied by difficulties associated with phase distortions introduced into the received signal by the atmosphere of our planet leading to a short coherent integration time.

These two key points have stimulated the development of multi-frequency synthesis (MFS) observation and data processing techniques. Observing in a multifrequency mode could improve (u, v)-coverage quality. Phase transfer (FPT) and source frequency phasereferencing (SFPR) methods could increase the coherent integration time by applying solutions from low frequencies to high frequencies (Rioja et al. 2011; Rioja & Dodson 2011; Rioja et al. 2017; Hodgson et al. 2016; Dodson et al. 2017).

MFS observations can be conducted simultaneously at all frequencies or quasi-simultaneously by switching frequencies. The Korean VLBI Network (KVN) is an excellent example of a simultaneous multifrequency VLBI system (Han et al. 2012; Rioja et al. 2015; Algaba et al. 2015; Han et al. 2017; Zhao et al. 2018, 2019; Yoo et al. 2021).

This promising multi-frequency observation mode was taken into account during the development of the Radioastron space observatory (Kardashev et al. 2013, 2015). It is, of course, true that Radioastron's regime cannot be described as a standard or familiar as we currently envision. The Astro Space Center has developed modern algorithms for processing such MFS observations (Likhachev 2005; Likhachev et al. 2006, 2009).

Thus, following the launch of the Radioastron, it was both necessary and critical to check the mode's operability and evaluate its capabilities. Below we summarize and discuss the results of the first such observation conducted with Radioastron.

2. Radioastron Space Observatory

Launched on 18 July 2011, Radioastron became the largest space radio telescope, with a 10 meter deployable parabolic antenna. Its operation lasted 2.5 times longer than expected, and ended in January 2019 (Kardashev et al. 2013, 2015).

The space radio telescope achieved a record angular resolution of 7 μas, thanks to its high elliptical near-Earth orbit with an apogee of 360000 km and an orbital period of 9 days. Radioastron observed in four frequency bands: 92 cm (316–332 MHz, P-band), 18 cm (1636–1692 MHz, L-band), 6.2 cm (4804–4860 MHz, C-band), and 1.2–1.6 cm (18372–25132 MHz, K-band).

The signal was recorded into two circular polarization channels (left-hand or LCP and right-hand or RCP) and an IF bandwidth of 2×16 MHz (upper and lower sub-bands).

Radioastron observed more than 300 radio sources with almost all ground radio telescopes across the world. Most of the observing time was devoted to the active galactic nuclei (AGN) survey (Kovalev et al. 2020; Kovalev 2021a,b), among other pulsars and galactic masers.

2.1. Onboard Multi-Frequency System

The space radio telescope had a switchable multifrequency system for the 1.3 cm (22 GHz) band. The receiver was designed to operate between 18 and 25 GHz (Andreyanov et al. 2007). Using two parallel channels with orthogonal circular polarization, it amplified, filtered, and double converted input noise signals with a continuous spectrum and spectral lines from the antenna irradiator into intermediate frequency signals (interferometric output). Using the superheterodyne method with double-frequency conversion, the receiving path was constructed. A low noise amplifier was used to achieve maximum sensitivity at the receiving tract's input.

There are eleven frequency channels with identical analysis bands on the receiving path. In MFS mode, the first heterodyne is switched between eight frequencies with a 960 MHz step. To ensure the "Synthesis" mode, one of the receiver channels operates with a fixed central frequency of 22236 GHz analysis bands ("Reference" channel), while in the second channel ("Switchable" channel) the bands are switched cyclically from a minimum of 18396 GHz to a maximum of 25116 GHz from the internal software temporary device. The transition between bands should not take longer than 10 seconds.

3. Observations

To test the Radioastron MFS mode, we scheduled and conducted a short-term observation in 2017 with the Korean Astronomy and Space Science Institute (KASI) and European observatories. As a target source, we selected 0059+581 (J0102+5824) (RA: $01^h2^m45^s.762$, DEC: $+58°24'11''.137$, J2000). It is a compact bright extra-galactic source with a flat spectrum classified as a blazar with a redshift $z = 0.644$ (Sowards-Emmerd et al. 2005) and estimated luminosity distance of 3844 Mpc.

It has a significantly variable flux density on short and long timescales, with signs of flare activity (Varenius et al. 2022). Several monitoring programs have observed it at radio, gamma, and optical wavelengths (Teräsranta et al. 2004; Pyatunina et al. 2006; Paliya et al. 2021).

Observation with code RATS01 was conducted on 14.01.2017 03:10–04:00 UTC, lasting 0.8 hours (48 minutes). The session entailed eight 360 second scans (one scan per frequency).

KVN antennas: Tanma (KT), Ulsan (KU), Yonsei (KY); Medicina (MC), and Torun (TR) participated as ground support for the space radio telescope. There were two circular polarization channels (RCP and LCP) for each telescope and two sub-bands, 16 MHz each. Observations covered frequencies from 18 to 25 GHz: 18396, 19356, 20316, 21276, 22236, 23196, 24156, and 25116. Frequencies are separated by 960 MHz. Figure 1 shows the frequency setup and switching. Radioastron, KT, KU, and KY switched from 21276 to 23196 MHz, TR observed at 22236 MHz, and MC observed from 18396 to 25116 MHz.

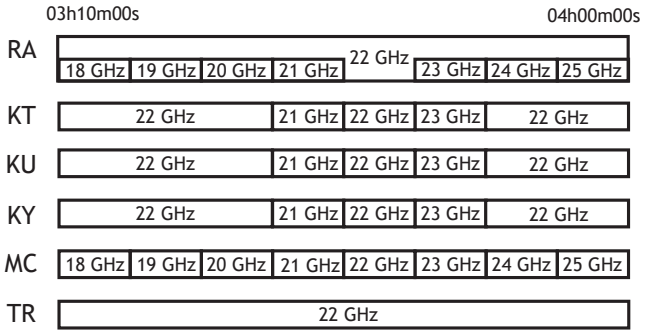

Figure 1. Time and frequency scheme of the RATS01 observation session. Radioastron (RA); KVN: Tanma (KT), Ulsan (KU), Yonsei (KY); Medicina, Italy (MC); Torun, Poland (TR).

Ground telescopes that switched frequencies did this in all channels. Radioastron observed in two channels: the "Reference" channel in RCP with a fixed frequency of 22236 MHz throughout all the scans of the observation and the "Switching" channel in LCP.

The space-ground interferometer configuration covered baseline projections of ~0.03, 0.5, 1.1–1.5 Earth Diameters (ED). The longest baseline corresponds to a maximum linear angular resolution of 0.19 mas. Figure 2 shows the resulting (u, v) coverage for all frequencies. The Radioastron observatory was at its perigee at the time of observations, and thus the space-ground baselines changed relatively quickly.

4. Data Reduction and Calibration

The raw data were collected and correlated in the Astro Space Center data processing center by ASC Software Correlator (Likhachev et al. 2017).

A standard algorithm for fringe search includes two correlation passes (Andrianov et al. 2019). The final correlation pass had 64 spectral channels and an integration time of 1/8 sec. Each frequency was processed separately.

In the next step, correlated VLBI data were calibrated, including amplitude calibration, bandpass calibration, and fringe fitting. Bandpass calibration was performed based on the telescope auto spectra. Amplitude calibration was done with observatory calibration tables. Both procedures were performed in the AIPS software package. The Medicina telescope was used as a reference antenna in a fringe fitting procedure by the Astro Space Locator (ASL) package Likhachev et al. (2020) with a solution interval of 360 seconds (six minutes) equal to a single scan.

Using the algorithms implemented in ASL software, we performed image synthesis in MFS mode after calibrating all the data. The following parameters were used:

- Field of view: 0.002×0.002 mas with the resolution of 512×512 pixels;

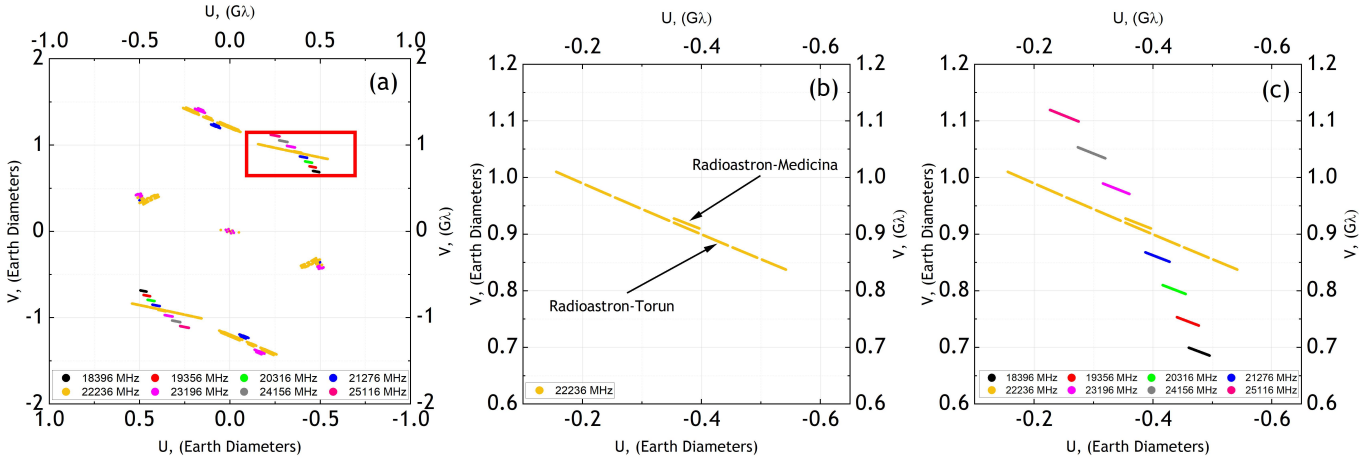

Figure 2. (u, v) coverage of RATS01 observation with Radioastron: (a) full (u, v) coverage with MFS; (b) magnified part of (u, v) coverage highlighted with a red rectangle on (a) (single frequency 22236 MHz), note: long track corresponds to Radioastron-Torun baseline, short track corresponds to Radioastron-Medicina baseline; (c) magnified part of (u, v) coverage highlighted with a red rectangle on (a) with MFS.

- Uniform weighting;
- Beam regularization was used to improve the image: because of the loose (u, v)-coverage there were significant sidelobes;
- The gridding procedure used a Gaussian kernel function with a full width at half magnitude FWHM = 1.5 of single cell width;
- Applied Gaussian tapering function;
- CLEAN method operated till the first negative component (~50 clean iterations);
- Central frequency for the image was set to F_c = 22220.25 MHz.

This approach is primarily explained by the rather loose (u, v) coverage.

5. Results

We obtained an image of 0059+581 with a 0.41×0.25 mas resolution (Figure 3 (left)). Due to the low dynamic range and the lack of (u, v)-coverage, the image does not demonstrate any details identified with a jet, as, for example, in the MOJAVE catalog[1] (Lister et al. 2021) or, for example, the data-sets discussed in Pyatunina et al. (2006).

Therefore, the image corresponds to the central core component (see Figure 3 (left)).

Integrated flux density and peak flux density were measured at 2.71 and 2.65 Jy/beam, respectively. The brightness temperature can be estimated using all the above values:

$$T_{\rm b} = 1.36 \frac{\lambda}{\theta_{\rm maj}\theta_{\rm min}} I \qquad (1)$$

where $T_{\rm b}$ is the brightness temperature (K), λ = 1.36 cm — observing wavelength, $\theta_{\rm maj} = 0.19 \times 10^{-3}$ as — Gaussian major axis, $\theta_{\rm min} = 0.11 \times 10^{-3}$ as — Gaussian minor axis, and $I = 2.65 \times 10^3$ mJy/beam — peak flux density. The lower limit for the brightness temperature was calculated using a minimum resolvable size of Gaussian $\theta_{\rm maj}$ = 0.19 mas, $\theta_{\rm min}$ = 0.11 mas. We obtained a limit of $T_{\rm b,lim} > 3.2 \times 10^{11}$ K. Referring to earlier measurements, for example, in Kovalev et al. (2005), where for 0059+581 the estimated core flux density at 15 GHz VLBA observations is 3.12 Jy with a resolution of 0.5 mas in the east-west direction and 0.6–1.3 mas in the north-south direction, the brightness temperature with a lower estimate $T_{\rm b} > 1.22 \times 10^{12}$ K with estimated $\theta_{\rm maj}$ = 0.13 mas and $\theta_{\rm min}$ = 0.11 mas. Most complete VLBA survey observations of 0059+581 at 15 GHz having 29 epochs demonstrated the minimum, medium, and maximum values of the brightness temperature to be as follows: $T_{\rm b,min} = 2.1 \times 10^{11}$ K, $T_{\rm b,med} = 1.9 \times 10^{12}$ K and $T_{\rm b,max} = 6.6 \times 10^{12}$ K correspondingly, the last session conducted in July 2013 yielded peak flux density of 2.5 Jy, $T_{\rm b} = 1.1 \times 10^{12}$ K (Homan et al. 2021).

The algorithms described in Likhachev (2005), Likhachev et al. (2006, 2009) and implemented in the Astro Space Locator VLBI data processing software package made it possible to obtain a spectral index map for the 18–25 GHz band (see Figure 3 (right)). The resulting spectral index map and spectral energy distribution shown in Figure 4 give an estimate of the spectral index α from $S_\nu \propto \nu^{-\alpha}$ for our observations $\alpha = -0.282 \pm 0.034$. This coincides with the results obtained earlier in Pyatunina et al. (2006); Fan et al. (2010); Hovatta et al. (2014). Accordingly, 0059+581 has noticeable variability, and the spectral index can also vary significantly based on the observation epoch. For example, in Pyatunina et al. (2006) two epochs of observations in a range from 0.8 to 1.6 GHz T = 2000.38 years and T = 2001.65 years gave for the core component values of the spectral index $\alpha = -1.14$ and $\alpha = -0.24$ correspondingly. According to the suggested explanation for spectral index variability, the decrease in optical depth of the source is related to an increase in core transparency. At the same time, later published results by Fan et al. (2010) include a wider data span from 1994 to 1999 providing an average spectral index for the core component $\alpha = -0.285$ stating that for most flat spectrum radio quasars their spectral

[1] https://www.cv.nrao.edu/MOJAVE/

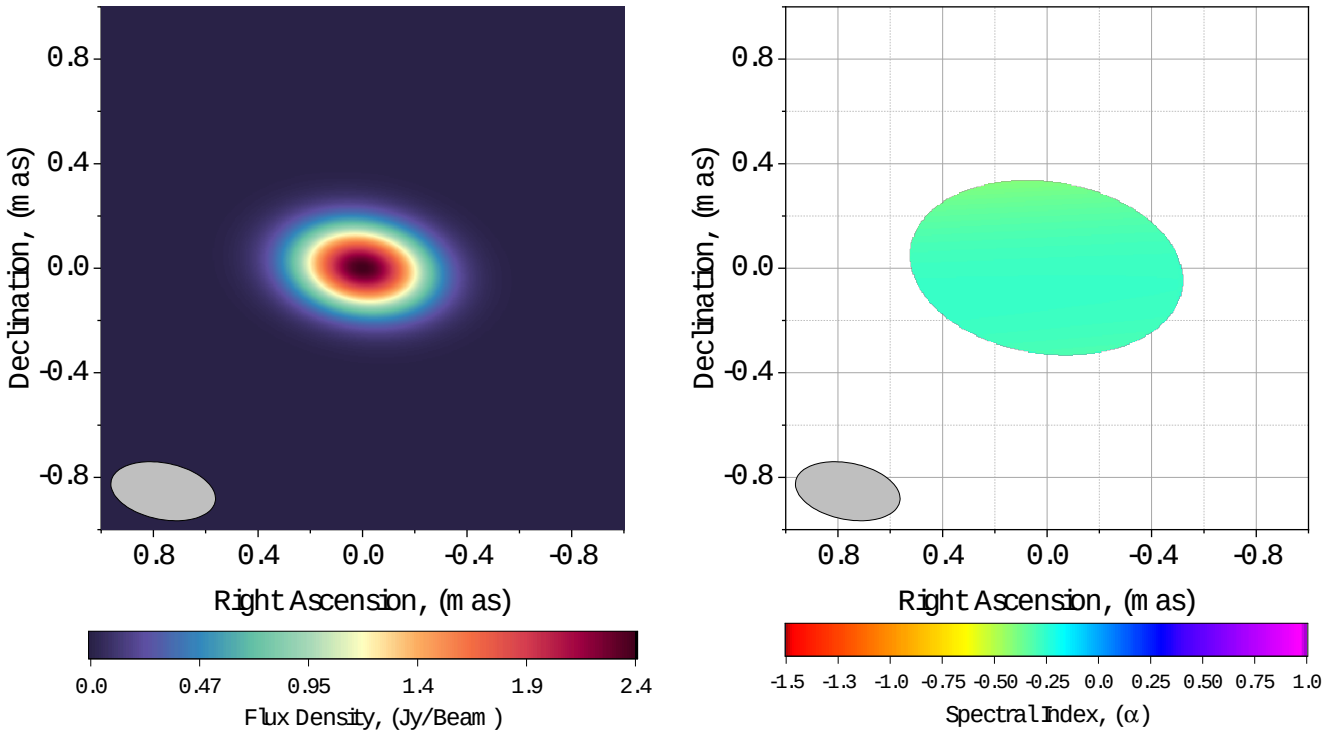

Figure 3. Synthesized image of 0059+581 (left) and spectral index distribution for 22200.2 MHz (right). Image center at RA: $01^{h}02^{m}45^{s}.8$, DEC: $58°24'11''.1$, beam size: 0.41×0.25 mas at 81.87°.

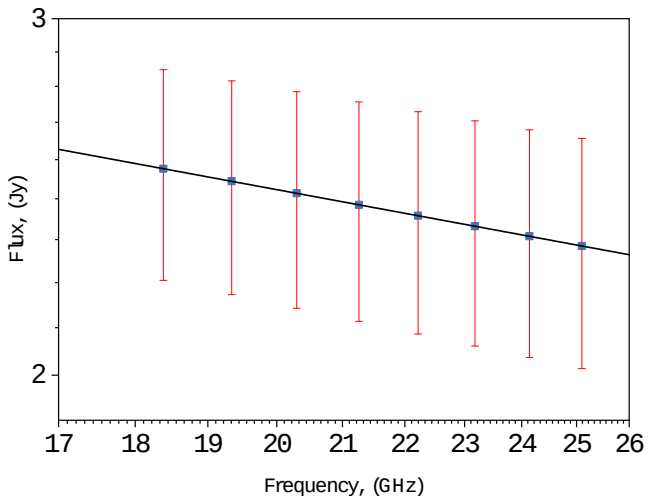

Figure 4. Spectral energy distribution measured by Radioastron space-Earth VLBI for 18–25 GHz frequency range in full log scale.

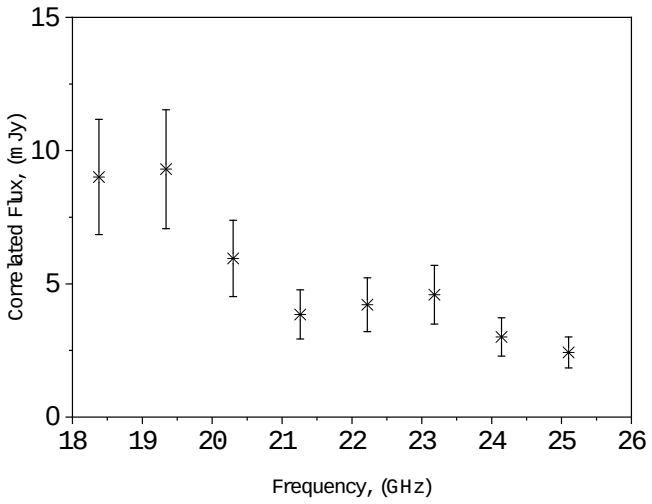

Figure 5. Correlated flux in mJy depending on the frequency range for RA-MC baseline.

indexes could lie and vary in the range from −1.0 to 1.0. Recent work Liu et al. (2018) showed the results of Effelsberg monitoring of a sample of RadioAstron blazars in terms of intra-day variability (IDV). The observations took an epoch with a total duration of 62 hrs, where the spectral index was measured for 0059+581 as $\alpha = -0.06$ and the peak flux density 3.52 Jy.

Using the Radioastron-Medicina baseline, we analyzed the correlated flux in frequency bands 18–25 GHz. Figure 5 shows that the flux distribution falls off with the increasing frequency, proving the performance and sensitivity of the Radioastron K-band receiver (see Figure 3 and Table 3 in Kovalev et al. (2014)). According to this work, the sensitivity of the space-ground interferometer in five sub-bands at wavelengths from 1.35 to 1.7 cm (18–22 GHz) can be up to 1.5 times higher, and in the following three sub-bands from 1.35 to 1.2 cm (22–25 GHz) up to 1.5 times lower than at 22 GHz. In our case, the decrease in correlated flux at 25 GHz compared to 18 GHz is almost two-fold. However, in the same work Kovalev et al. (2014), the sensitivity estimation errors for a 1.35 cm receiver are about 20–25%. According to our observations in 2017, the receiver's performance, measured in 2011–2013, is within acceptable limits.

6. Conclusions

We conducted the first space-ground VLBI MFS observations with Radioastron. It was the first time the space radio telescope used the "Reference" and "Switchable" channels. The data were processed with MFS algorithms implemented in the ASL Software package.

While the session was short, an image of the core component was obtained at central frequency 22220.5 MHz. This image had a beam resolution of 0.41×0.25 mas. Measured peak and integral flux density amounted to 2.65 Jy/beam and 2.71 Jy, respectively, and we estimated the lower limit for brightness temperature to be $T_{\mathrm{b,min}} > 3.2 \times 10^{11}$ K. The algorithms for MFS data processing made it possible to obtain information about the spectral index for 0059+581: $\alpha = -0.282 \pm 0.034$.

In addition, a secondary task was to evaluate the sensitivity and efficiency of the 1.35 cm receiver in a wide range of 18–25 GHz, which, taking into account measurement errors and previous estimates, confirms a significant drop in sensitivity in the higher-frequency (22–25 GHz) part of the receiver's operating bandwidth, and at the same time indicates a relatively stable state of the receiver compared between 2011–2013 and 2017.

All these results turned out to be quite reasonable, and we can conclude that such a regime of Radioastron observations validated its feasibility and operability, but also revealed its advantages and disadvantages, which is an essential part of the conclusion from the mission results. A mode like this would allow one to measure a number of parameters, for example, of AGN, in a relatively short time. It would also improve (u, v)-coverage, and calibrate phase using "Reference" and "Switching" channels. The main drawback was the lack of ground telescopes compatible with such a mode. No telescope on Earth could observe both the "Reference" and "Switching" channels in the same way as Radioastron. As a result, the phase calibration could not be profiled based on the "Reference" channel. The frequency switching mode was the only fully tested mode.

All of this leads to an important conclusion. Both on Earth and in space, VLBI is developing rapidly towards millimeter wavelengths. There are acute issues of improving (u, v)-coverage, which is especially critical for space-space and space-ground VLBI and phase calibration at higher frequencies. And in this case, MFS observations and data reduction technology can certainly solve both problems at the same time. The operating range of the 1.35 cm receiver was already relatively narrow at the time of Radioastron's launch for real improvement of the (u, v)-coverage. This is due to the fact that this range of switched frequencies within the (u, v) plane scales gives an advantage that is much smaller than the gaps, which are largely caused by the Radioastron high elliptical orbit configuration. However, the experience of Radioastron's observations presented in this article cannot be called in vain. Obviously, it demonstrates that MFS itself could increase the potential of VLBI observations and improve (u, v)-coverage (e.g., Likhachev et al. 2020).

Thus, taking into account modern realities, simultaneous observation in several bands will certainly become a full-fledged MFS, as in KVN, for example. This experience should be considered when planning any future VLBI mission, whether it is space-space, space-ground or ground-based. Studies in this area are already underway, as part of the extended-KVN and ngEHT projects, as well as the development of the Millimetron space observatory (Dodson et al. 2016; Raymond et al. 2021; Likhachev et al. 2022; Rudnitskiy et al. 2022).

Acknowledgments

The RadioAstron project was led by the Astro Space Center of the Lebedev Physical Institute of the Russian Academy of Sciences and the Lavochkin Scientific and Production Association under a contract with the State Space Corporation ROSCOSMOS, in collaboration with partner organizations in Russia and other countries.

This work is based on observations carried out using Korean VLBI Network antennas operated by Korean Astronomy and Space Science Institute (KASI).

It is partly based on observations with the Medicina (Noto) telescope operated by INAF — Istituto di Radioastronomia.

This work is also based in part on observations carried out using the 32-meter radio telescope operated by Torun Centre for Astronomy of Nicolaus Copernicus University in Torun (Poland) and supported by a Polish Ministry of Science and Higher Education SpUB grant.

References

Algaba, J.-C., Zhao, G.-Y., Lee, S.-S., et al. 2015, JKAS, 48, 237

Andreyanov, V. V., Biriukov, A. V., Vasil'Kov, V. I., et al. 2007, in Radioastronomical Tools and Techniques, ed. N. S. Kardashev & S. A. Dagkesamanskii, 17

Andrianov, A. S., Guirin, I. A., Kostenko, V. I., et al. 2019, in ASP Conf. Ser., Vol. 521, Astronomical Data Analysis Software and Systems XXVI, ed. M. Molinaro, K. Shortridge, & F. Pasian, 323

Dodson, R., Jung, T., Rioja, M., et al. 2016, in URSI Asia-Pacific Radio Science Conference (URSI AP-RASC), 44

Dodson, R., Rioja, M. J., Molina, S. N., & Gómez, J. L. 2017, ApJ, 834, 177

Fan, J.-H., Yang, J.-H., Tao, J., Huang, Y., & Liu, Y. 2010, PASJ, 62, 211

Han, S.-T., Lee, J.-W., Lee, B., et al. 2017, J Infrared Millim Terahertz Waves, 38, 1487

Han, S. T., Lee, J. W., Kang, J., et al. 2012, in Proc. of the 11th European VLBI Network Symposium & Users Meeting. 9-12 October, 59

Hodgson, J. A., Lee, S.-S., Zhao, G.-Y., et al. 2016, JKAS, 49, 137

Homan, D. C., Cohen, M. H., Hovatta, T., et al. 2021, ApJ, 923, 67

Hovatta, T., Aller, M. F., Aller, H. D., et al. 2014, AJ, 147, 143

Kardashev, N. S., Alakoz, A. V., Kovalev, Y. Y., et al. 2015, Sol. Syst. Res., 49, 573

Kardashev, N. S., Khartov, V. V., Abramov, V. V., et al. 2013, Astron. Rep., 57, 153

Kovalev, Y. 2021a, in 43rd COSPAR Scientific Assembly. Held 28 January – 4 February, Vol. 43, 1435

Kovalev, Y. 2021b, in Nuclear Activity in Galaxies Across Cosmic Time, ed. M. Pović, P. Marziani, J. Masegosa, H. Netzer, S. H. Negu, & S. B. Tessema, Vol. 356, 256
Kovalev, Y. A., Vasil'kov, V. I., Popov, M. V., et al. 2014, Cosm. Res., 52, 393
Kovalev, Y. Y., Kellermann, K. I., Lister, M. L., et al. 2005, AJ, 130, 2473
Kovalev, Y. Y., Kardashev, N. S., Sokolovsky, K. V., et al. 2020, Adv. Space Res., 65, 705
Likhachev, S. 2005, in ASP Conf. Ser., Vol. 340, Future Directions in High Resolution Astronomy, ed. J. Romney & M. Reid, 608
Likhachev, S., Kogan, L., Fomalont, E., & Owen, F. 2009, in ASP Conf. Ser., Vol. 402, Approaching Micro-Arcsecond Resolution with VSOP-2: Astrophysics and Technologies, ed. Y. Hagiwara, E. Fomalont, M. Tsuboi, & M. Yasuhiro, 444
Likhachev, S. F., Kostenko, V. I., Girin, I. A., et al. 2017, J. Astron. Instrum., 6, 1750004
Likhachev, S. F., Ladygin, V. A., & Guirin, I. A. 2006, Radiophys. Quantum Electron., 49, 499
Likhachev, S. F., Rudnitskiy, A. G., Shchurov, M. A., et al. 2022, MNRAS, 511, 668
Likhachev, S. F., Girin, I. A., Avdeev, V. Y., et al. 2020, Astron. Comput., 33, 100426
Lister, M. L., Homan, D. C., Kellermann, K. I., et al. 2021, ApJ, 923, 30
Liu, J., Bignall, H., Krichbaum, T., et al. 2018, Galaxies, 6, 49
Paliya, V. S., Ajello, M., Cao, H. M., et al. 2021, VizieR Online Data Catalog, J/ApJ/897/177
Pyatunina, T. B., Gabuzda, D. C., Jorstad, S. G., et al. 2006, Astron. Rep., 50, 468
Raymond, A. W., Palumbo, D., Paine, S. N., et al. 2021, ApJS, 253, 5
Rioja, M., & Dodson, R. 2011, AJ, 141, 114
Rioja, M., Dodson, R., Gómez, J., et al. 2017, Galaxies, 5, 9
Rioja, M., Dodson, R., Malarecki, J., & Asaki, Y. 2011, AJ, 142, 157
Rioja, M. J., Dodson, R., Jung, T., & Sohn, B. W. 2015, AJ, 150, 202
Rudnitskiy, A. G., Mzhelskiy, P. V., Shchurov, M. A., Syachina, T. A., & Zapevalin, P. R. 2022, Acta Astron., 196, 29
Sowards-Emmerd, D., Romani, R. W., Michelson, P. F., Healey, S. E., & Nolan, P. L. 2005, ApJ, 626, 95
Teräsranta, H., Achren, J., Hanski, M., et al. 2004, A&A, 427, 769
Varenius, E., Maio, F., Le Bail, K., & Haas, R. 2022, Exp. Astron., 54, 137
Yoo, S., Lee, S.-S., Kim, S.-H., & An, H. 2021, J. Astron. Space Sci., 38, 193
Zhao, G.-Y., Algaba, J. C., Lee, S. S., et al. 2018, AJ, 155, 26
Zhao, G.-Y., Jung, T., Sohn, B. W., et al. 2019, JKAS, 52, 23